Oxidation of Metals, Vol. 23, Nos. 1/2, 1985

Effect of Cold Work on the Oxidation Resistance of $2\frac{1}{4}$ Cr–1 Mo Steel

A. S. Khanna* and J. B. Gnanamoorthy*

Received May 30, 1984; Revised August 10, 1984

The effect of cold work on the oxidation rate of $2\frac{1}{4}$ Cr–1 Mo steel in pure oxygen at 1 atm pressure at temperatures ranging from 400 to 950°C has been studied for short exposure periods (max. 4 hr). The specimens had been cold worked up to 90% by cold rolling. The results indicate negligible effect of cold work on the oxidation kinetics up to 700°C, beyond which there is general reduction in oxidation. The effect was pronounced at 900°C. The increased resistance to oxidation has been attributed to the faster diffusion of chromium in the cold-worked material compared to the annealed one, leading to the formation of a chromium-rich spinel which helps in slowing down the oxidation of the alloy. The findings have been corroborated by the examination of all samples oxidized at 900°C by optical, EPMA, SEM, and EDAX analyses.

KEY WORDS: Cold work; oxidation; spinel; $2\frac{1}{4}$ Cr–1 Mo steel.

INTRODUCTION

The effect of cold work on the oxidation of various ferrous alloys in different atmospheres has been studied by several workers. The results indicate that in the case of iron,[1–3] the effect is detrimental while prior cold work in several iron-chromium alloys[4] and stainless steel[5,6] enhances the oxidation resistance of these alloys. Oxidation resistance of an Fe–10% Cr alloy at 600°C in air increases with increasing amounts of cold work in the alloy.[7] Breakaway oxidation can be prevented till at least 2000 hr at 600°C for this

*Materials Development Laboratory, Reactor Research Centre, Kalpakkam-603102, Tamilnadu, India.

0030-770X/85/0200-0017$04.50/0

alloy by severe cold rolling.[8] Caplan[4] reported that cold work increases the oxidation of 10–16 wt.% Cr alloys, but decreases the oxidation rate of higher Cr alloys.

In pure iron, it has been proposed[1–3] that the oxidation rate increases because of better scale adhesion, which increases the scaling rate, and in the case of iron-chromium alloys, the enhancement of oxidation resistance has been attributed to the faster diffusion of chromium, which forms the protective scale.[4,9] Recent work has shown that oxidation behavior of Fe–Cr and Ni–Cr alloys depends on the distribution of Cr and on certain microstructural features in the oxide.[7] Little information is available on the oxidation behavior of low-chromium steels. The present work reports the results of oxidation studies on an industrially important low-chromium alloy, viz., $2\frac{1}{4}$ Cr–1 Mo steel.

EXPERIMENTAL METHOD

Sheets of $2\frac{1}{4}$ Cr–1 Mo steel, 6 mm thick, whose chemical composition is given in Table I, were used as the starting material for the studies. Strips $60 \times 10 \times 3$ mm were cut from these sheets and cold rolled to a thickness of approximately 1 mm. They were then sealed in an evacuated quartz tube and were heat treated at 950°C for 2 hr. Taken as 0% cold-worked samples, the strips were then used to obtain samples with different degrees of cold work by cold rolling. Thus specimens with cold work of 37%, 46%, 63%, 76%, and 89% were prepared. Rectangular samples with total surface area of 1–2 cm^2 were cut from these strips and were polished to submicron finish using a series of SiC papers and diamond paste, degreased, and finally washed in alcohol before use. Oxidation was carried out in oxygen purified from moisture and carbon dioxide at 1 atm pressure for a fixed duration of 4 hr at temperatures ranging from 400 to 950°C, in a Mettler TA1 thermoanalyser. A ramp heating program of 25°C/min was used to reach the desired temperature. For kinetic calculations, zero time has been taken only after the desired temperature was reached. Postoxidation studies were carried out using EDAX and EPMA for determining surface oxide composition and concentration profiles through the oxide/alloy layer.

Table I. Nominal Chemical Composition of Steel Used

Element	Cr	C	Mn	Si	P	S	Mo	Cu	Ni	Fe
Wt.%	2.28	0.07	0.42	0.019	0.19	0.025	0.95	0.03	0.08	Bal.

EXPERIMENTAL RESULTS

Kinetics

The total weight gain observed after a fixed duration of 4 hr oxidation on various cold-worked samples at various temperatures is given in Table II. Weight-gain data indicate negligible effect of cold work on oxidation up to 700°C. At higher temperatures, the effect was found to be significant. The data for 800, 900, and 950°C are plotted in Fig. 1. The effect of cold work on oxidation behavior seems to follow a similar trend at all the three temperatures. There is a general decrease in the weight gain as the cold work increases. However, a slight increase in weight gain at about 46% cold work is noted, and is being investigated further.

The effect of cold work on oxidation kinetics can be depicted by the linear weight-gain plots at various temperatures as shown in Figs. 2, 3, and 4. At 800°C the decrease in weight gain is due to the decrease in parabolic rate constants calculated from the square of the weight gain versus time plot (top left of Fig. 2) and listed in Table III. At 900°C, breakaway oxidation was observed in annealed samples, but no breakaway was seen in cold-worked samples. This is quite evident from the total weight-gain data given in Table II as well as from the plots of the square of the weight gain versus time (top left of Fig. 3). As seen from Table III, the parabolic rate constants for the cold-worked samples generally decrease with increased cold work. At 950°C, breakaway oxidation was observed on all the cold-worked samples. Therefore, the decrease in the total weight gains with increased levels of prior cold work is due to the decrease in the postbreakaway rates of oxidation: from 1.05 $\mu g/mm^2/min$ for the annealed sample to 0.938,

Table II. Total Weight Gain in $\mu g/mm^2$ in 4 hr Isothermal Oxidation at Various Temperatures

		Cold-worked					
Temp. (°C)	Fully annealed 0%	37%	46%	59%	63%	76%	89%
400	2.01	2.57	2.04		1.75	1.99	
500	3.63	4.60	3.34		3.86	4.45	
600	5.46	4.68	4.72		4.32	5.78	
700	11.67	10.93	10.83		10.45	11.8	
800	30.04	22.96	26.50		19.70	19.60	
900	178.75	78.12	86.71	73.88	62.90	54.50	32.54
950	349.50	301.76	326.52		285.9	281.40	

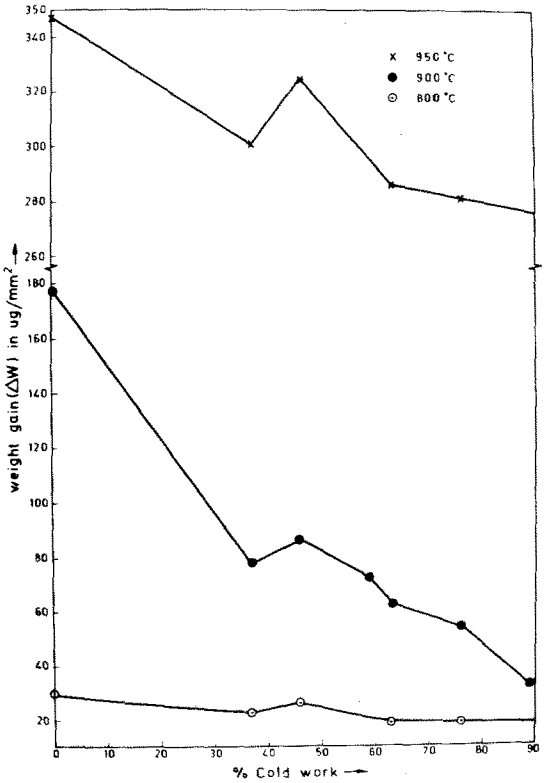

Fig. 1. Total weight gain during 4 hr oxidation as a function of degree of cold-work at various temperatures.

Table III. Parabolic Rate Constants for Various Cold-Worked Samples at Different Temperatures

%	Parabolic rate constant ($\mu g^2\ mm^{-4}\ min^{-1}$)		
	800°C	900°C	950°C
0	3.83	*a*	*a*
37	1.85	27.8	*a*
46	1.35	27.8	*a*
63	1.31	5.5	*a*
76	1.31	5.5	*a*

[a] Breakaway oxidation.

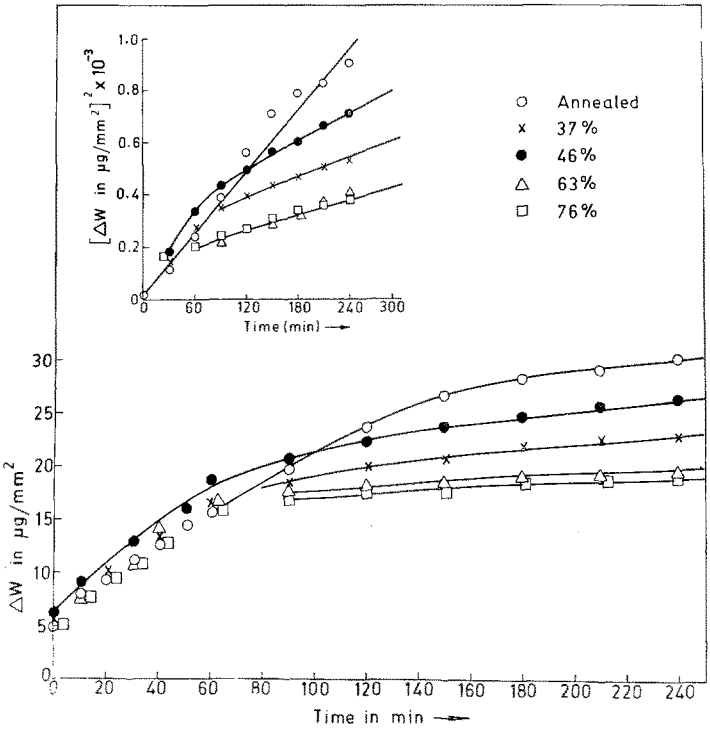

Fig. 2. Weight gain vs time plot and square of weight gain vs time plot (top left) at 800°C for 4 hr for different degrees of cold work.

0.794, 0.762, and 0.714 $\mu g/mm^2/min$ for 37%, 46%, 63%, and 73% cold work, respectively.

Oxide Scale Analysis

A detailed analysis of the oxidized surface of the steel was carried out on the samples oxidized at 900°C for 4 hr.

Surface Topography

Surface topographical features observed using SEM show blocky oxide masses and presence of cracks on the annealed sample (Fig. 5a), indicating an excessive oxidation compared to the uniform oxide layer with flowering types of oxide particles present on cold-worked samples (Fig. 5b for 76% cold-worked and Fig. 5c for 89% cold-worked samples). This is in conformity with the trend shown by the weight gain data discussed in the previous section. X-ray diffraction analysis carried out on these samples indicated

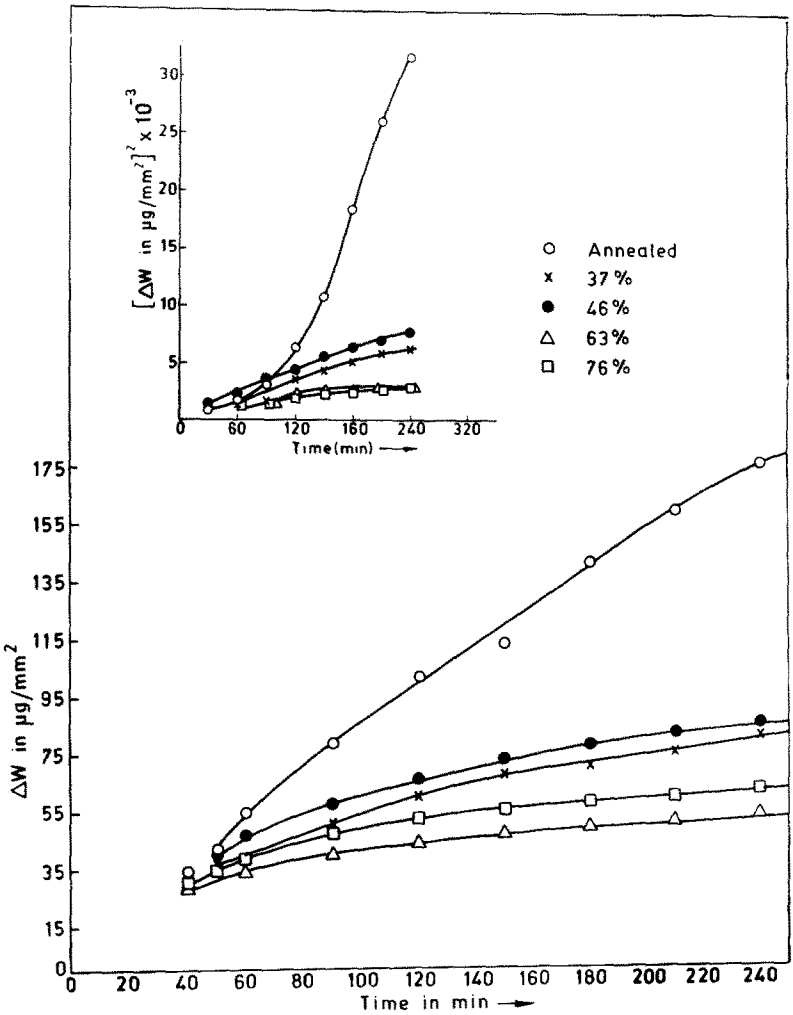

Fig. 3. Some as Fig. 2 but at 900°C.

an α-Fe_2O_3 outer layer on the annealed sample and Fe_3O_4 on the cold-worked samples.

Cross-Section of the Oxide Scale

Oxide cross-section was studied using optical microscopy, SEM, EDAX, and EPMA. Figure 6 shows the SEM micrographs of the oxide scale along with the elemental distribution of the various constituents of

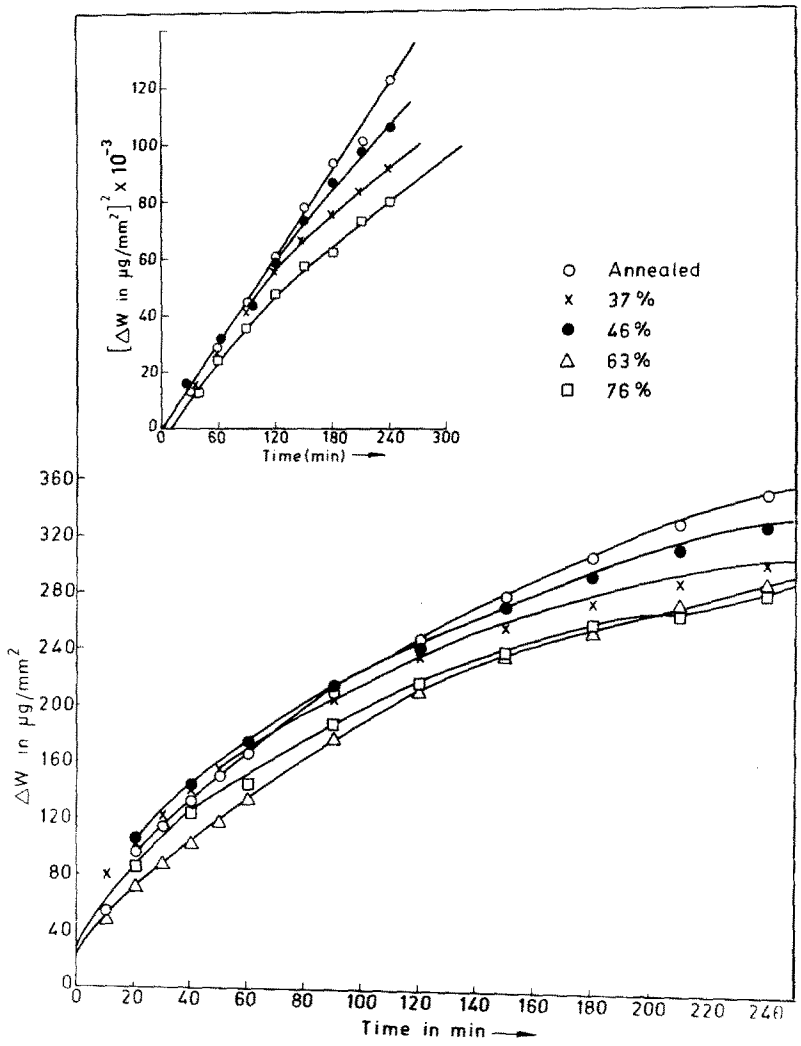

Fig. 4. Same as Fig. 2 but at 950°C.

the alloy in the oxide scale, measured by the point-to-point analysis technique using EDAX. It is clear from these micrographs that the oxide layer becomes thinner with the presence of prior cold work on the sample. Some of the other important features observed are as follows.

The outer scale formed on the annealed sample is very uniform and is brittle near the alloy/oxide interface. The scale formed on the cold-worked samples is relatively porous and is more so near the alloy/oxide interface.

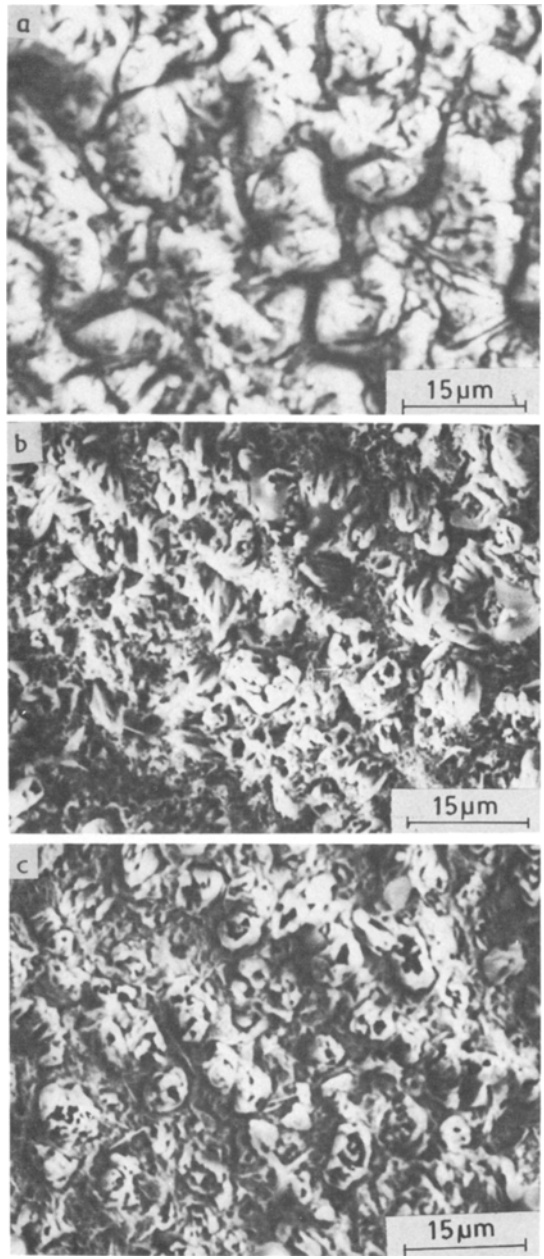

Fig. 5. SEM micrographs showing the surface topography of the oxide layer formed on (a) annealed specimen, (b) 63% cold-worked specimen, and (c) 89% cold-worked specimen during 4 hr oxidation at 900°C.

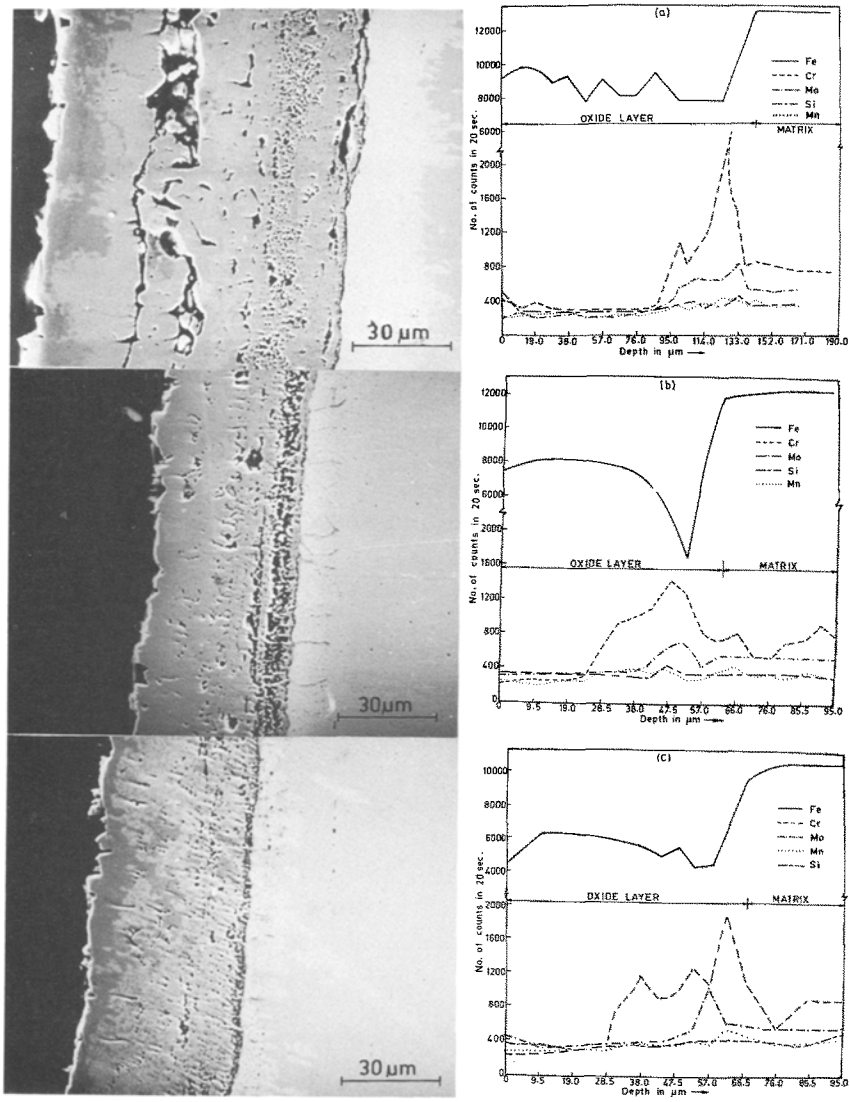

Fig. 6. Oxide cross-section (SEM micrograph) and depth profile for various constituent elements in (a) annealed specimen, (b) 37% cold-worked specimen, and (c) 46% cold-worked specimen during 4 hr oxidation at 900°C.

An additional feature on the cold-worked samples, which distinguishes it from the annealed samples, is the region in the unoxidized alloy matrix next to the alloy/oxide interface. This region consists of dark spots. Nital etch showed that these spots appear both within the grains and on the grain

boundaries (Fig. 7). EDAX analysis of these spots revealed that these are Cr-rich phases similar in composition to that of the oxide layer adjacent to the alloy/oxide interface. The Cr content at the grain boundaries is slightly more than that of the spots within the grains (Fig. 8). Thus it can be inferred that these spots represent the internal oxides formed in the alloy matrix adjacent to the alloy oxide interface.

Results of the EPMA analysis of the cross-section of the oxidized samples are shown in Fig. 9, which gives absorbed electron pictures of the scale as well as X-ray images of Cr and Fe. The absorbed electron picture shows a single layer on the annealed sample, while the pictures for cold-worked samples show a duplex layer. The X-ray images of Cr for cold-worked samples clearly show the regions of high Cr concentration within the alloy adjacent to alloy/oxide interface. These enriched phases are absent in the annealed samples. This is in agreement with the EDAX results given above.

Fig. 7. Optical micrograph showing the formation of internal oxides both within and on the grain boundaries (Nital etch) on a 37% cold-worked sample oxidized for 4 hr at 900°C.

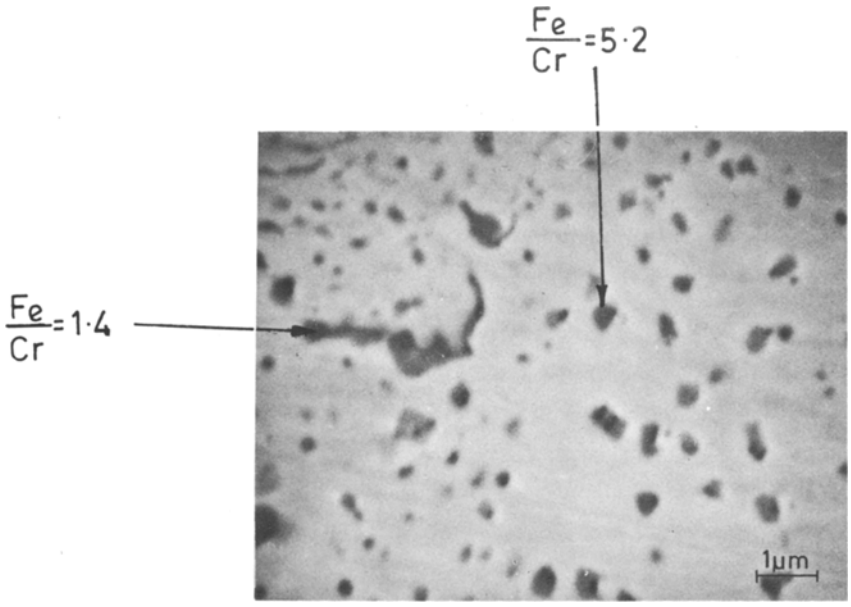

Fig. 8. SEM micrograph showing the internal oxide particles formed on the matrix adjacent to the oxide/metal interface.

The presence of duplex layers on the cold-worked samples was confirmed by the following special etching technique, which can distinguish an internal spinal layer from an outer iron-oxide layer on $2\frac{1}{4}$ Cr–1 Mo steels.[10] Anodic etching (using the specimen as the anode in 0.5% Na_2CrO_4 solution) will reveal the inner spinel layer (i.e., the layer adjacent to alloy/oxide interface) by the darkening in color; while cathodic etching (using the specimen as the cathode in 0.5% Na_2CrO_4 solution) will delineate the grain structure of the outer Fe_3O_4 oxide layer. Figure 10 gives the photomicrographs of the annealed and cold-worked samples (a) without etching, (b) anodically etched, and (c) cathodically etched. It is clearly seen from these micrographs that the cold-worked specimens show a dark, inner layer when anodically etched and an outer, delineated grain-boundary structure when cathodically etched. No such features are revealed in annealed specimens.

DISCUSSION

Both the thermogravimetric results and the oxide analysis discussed in the earlier sections demonstrate that the presence of prior cold work in the samples increases the oxidation resistance of $2\frac{1}{4}$ Cr–1 Mo steel at 800, 900,

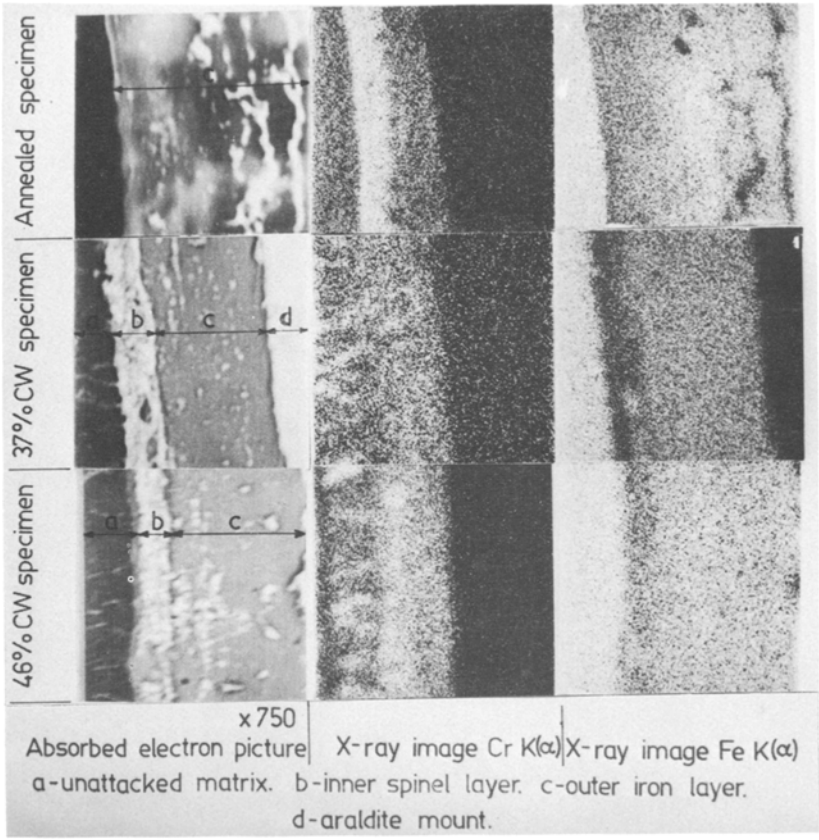

Fig. 9. Absorbed electron image and X-ray images of Cr and Fe obtained in the EPMA analysis of oxide layers of specimens oxidized at 900°C for 4 hr with different degrees of cold-worked (0%, 37%, 46%).

and 950°C. Detailed oxide-scale analysis at 900°C can be used to formulate a possible mechanism of this enhanced oxidation resistance. As compared to the annealed sample, two additional features have been observed in the cold-worked sample: (i) the presence of an internal oxide in the underlying matrix adjacent to the alloy/oxide interface and (ii) the duplex nature of the oxide scale consisting of an internal spinel layer and an outer Fe_3O_4 layer.

The presence of an internal spinel layer on iron–chromium alloys having $\leq 5\%$ of Cr has been reported by Wood.[11] Also it is well-known that a spinel structure is comparatively defect free when compared to a simple rhombohedral Fe_2O_3, Cr_2O_3 mixed oxide, which is believed to have been formed on the annealed sample. The presence of an internal spinel layer

thus reduces the transport of Fe to the outer surface, while the inward diffusion of oxygen is not affected, and therefore, more oxygen diffuses into the matrix through this spinel layer, resulting in the formation of internal Cr-rich mixed oxides. The question that still remains to be clarified is: What makes cold-worked samples form a duplex layer, which is not possible on the annealed alloy? Several workers[4,7,12] have reported that in iron-chromium alloys having $Cr \geq 9$ wt.%, the presence of prior cold work enhances Cr diffusion, which results in the formation of a more protective chromium oxide layer on the surface, thereby enhancing the oxidation resistance. Some workers[12,13] have proposed that fast diffusion of Cr occurs through some short-circuit diffusion paths in the underlying alloy which forms as a result of prior cold work in the specimens. The possibility of forming a chromium oxide layer does not exist in the present low-Cr alloy. However, a spinel layer is formed which is freer of defects than a simpler rhombohedral mixed oxide of Fe and Cr and hence helps in reducing the oxidation rate.

On the basis of these considerations, a mechanism has been formulated which is shown schematically in Fig. 11. The single layer consisting of a mixed oxide of Fe and Cr has been assumed to have formed on the annealed sample in the following way. In the initial stage of oxidation an iron oxide, Fe_2O_3, is formed along with an amount of Cr_2O_3 commensurate with the alloy composition. This layer ultimately grows to a mixed oxide of iron and chromium through the inward diffusion of oxygen ions and the outward diffusion of cations (Fe and Cr). Slow diffusivity of Cr results in its concentration at the alloy/oxide interface, and the outer layer grows as an oxide of iron, Fe_2O_3 (Fig. 11a and b). In the cold-worked samples, the initial stage of oxidation is similar to that of the annealed alloy with respect to the formation of a mixed oxide. As the oxidation progresses, the diffusion processes set in.

Due to the increased defect concentration in the cold-worked alloy, Cr diffuses faster towards the surface, and the higher concentration of Cr thus available at the alloy/oxide interface will lead to the formation of a spinel of the type $Fe_{2-x}Cr_xO_4$. After the formation of a complete layer of this spinel, further oxidation will be controlled by the diffusion of the cations and oxygen through this layer.[12] Diffusion of Cr through this spinel layer is comparatively slow.[14] This leads to the observed Cr enrichment in the spinel layer at the interface with the alloy. As a consequence, the diffusivity of Fe is also reduced,[15] thus lowering the overall oxidation rate. Hence, the diffusion of Fe through the spinel is assumed to be the rate-controlling step. The diffusivity of oxygen anions inward is, however, unaffected by the formation of this spinel layer and therefore causes internal oxidation in the underlying alloy (Fig. 11c, d, and e).

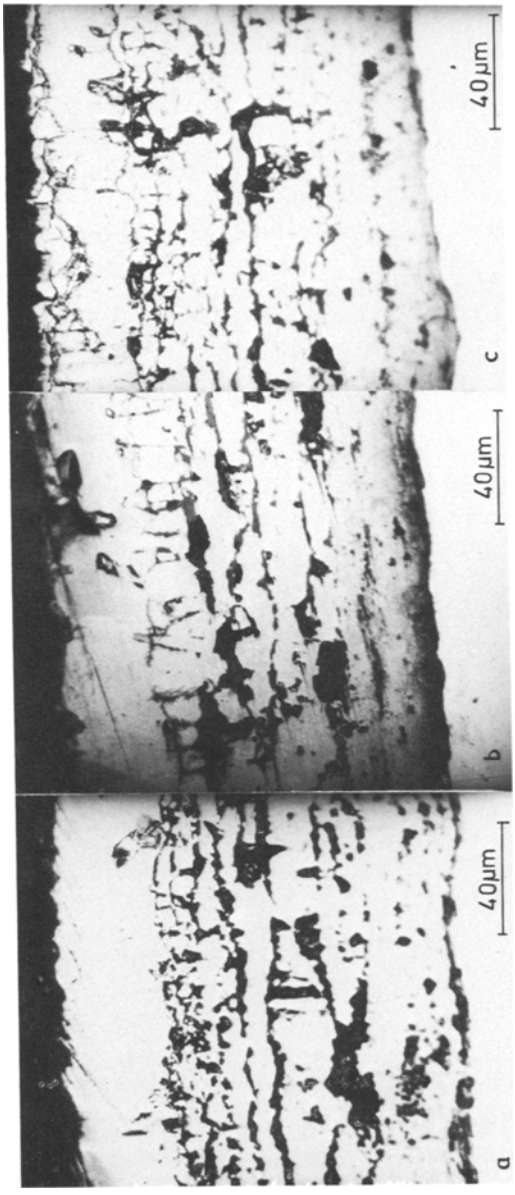

ANNEALED SAMPLE

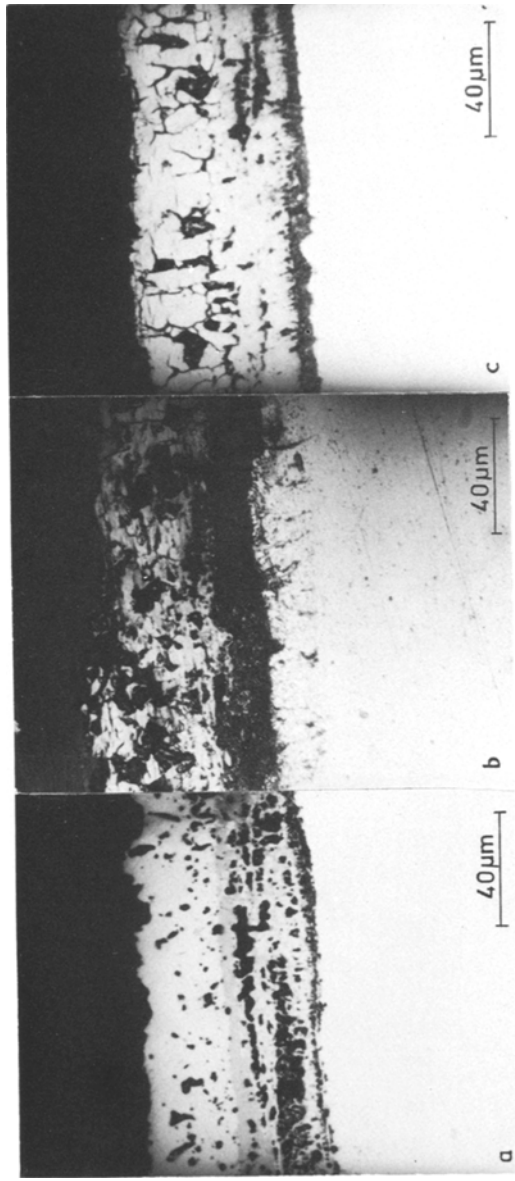

Fig. 10. Optical micrograph of oxide cross-section formed on annealed and 37% cold-worked sample under (left) without etch condition, (middle) anodic etching using 0.5% Na_2CrO_4 solution, and (right) cathodic etching using 0.5% Na_2CrO_4 solution. Samples oxidized for 4 hr at 900°C.

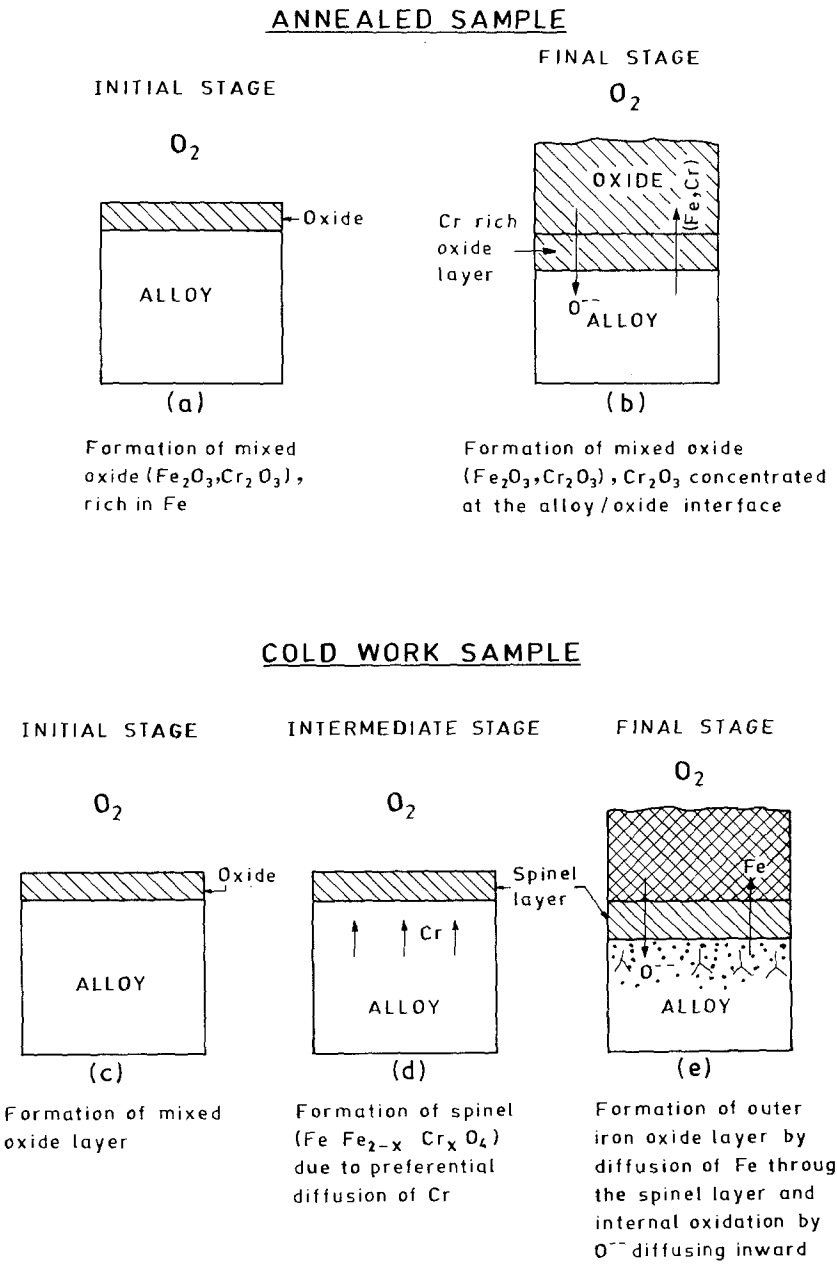

Fig. 11. Schematic diagram of formation of the scale.

CONCLUSIONS

The presence of prior cold work did not affect the oxidation rate of $2\frac{1}{4}$ Cr–1 Mo steel during a 4 hr exposure in pure oxygen up to 700°C. At 800°C and above, the presence of prior cold work decreased the general oxidation in the 4 hr exposure period in pure oxygen. This effect was most pronounced at 900°C. Enhancement in oxidation resistance in the cold-worked samples has been attributed to the formation of an inner spinel layer which reduces the rate of transport of cations.

ACKNOWLEDGMENTS

The authors gratefully acknowledge the assistance provided by S. Vaidynathan and P. Kuppuswamy of the Metallurgy Programme in examining the specimens by SEM/EDAX and X-ray diffraction, respectively.

REFERENCES

1. D. Caplan and M. Cohen, *Corr. Sci.* **6**, 321 (1966).
2. D. Caplan, G. I. Sproule, and R. J. Hussey, *Corr. Sci.* **10**, 9 (1970).
3. W. R. Price, *Corr. Sci.* 7, 473 (1967).
4. D. Caplan, *Corr. Sci.* **6**, 509 (1966).
5. W. E. Ruther and S. Greenberg, *J. Electrochem. Soc.* **111**, 116 (1964).
6. M. Warzee *et al.*, *J. Electrochem. Soc.* **112**, 670 (1965).
7. M. K. Hossain, *Corr. Sci.* **19**, 1031 (1979).
8. B. Kent and J. Davidson, *Micro '74 Supplement, Proc. RMS*, 9(4), 74 (1974).
9. K. C. Tripathi and J. E. Antill, *Corr. Sci.* **10**, 273 (1970).
10. M. H. Hurdus and L. Tomlinson, *Br. Corr. J.* **13**, 158 (1978).
11. G. C. Wood, *Corr. Sci.* **2**, 173 (1961).
12. G. O. Lloyd, S. R. J. Saunders, B. Kent, and A. Fursey, *Corr. Sci.* **17**, 269 (1977).
13. G. B. Gibbs and R. Hales, Proc. Conf. 'Point defect behavior and diffusional processes,' The Metal Society, University of Bristol (Sept. 1976), p. 201.
14. M. G. C. Cox, B. McEnaney, and V. D. Scott, *Philos. Mag.* **26**, 839 (1972).
15. D. P. Whittle and G. C. Wood, *J. Electrochem. Soc.* **114**, 986 (1967).